Kink Bands and Deformation in Graphite

Michel W. Barsoum[1], Anand Murugaiah[1], Surya R. Kalidindi[1] and Yury Gogotsi[1]

[1] *Department of Materials Science and Engineering, Drexel University, Phila., PA 19104*

Corresponding author e-mail address:barsoumw@drexel.edu

Introduction

True understanding of the deformation of graphite has resisted interpretation since the inception of the field [1]. For example, graphite exhibits reversible hysteretic stress strain loops (Fig. 1), the underlying mechanisms of which have to date not been clearly understood. In this paper we present compelling evidence based on spherical nanoindentations experiments on graphitic single crystals [2] and compression of bulk graphite samples that incipient kink bands that are *fully* reversible at low stresses, that give way to mobile dislocation walls at intermediate loads, that, in turn, collapse into kink boundaries at the highest loads can account for all our observations. As important much of the literature on the mechanical properties of graphite – especially the changes in moduli with load and microstructure etc. – are can be also explained by invoking the formation of kink bands.

Because the dislocations are confined to the basal planes, they do not entangle and can thus move reversibly over relatively large distances resulting in the dissipation of large amounts of (up to 100 MJ/m^3) energy during each cycle. The energy dissipated

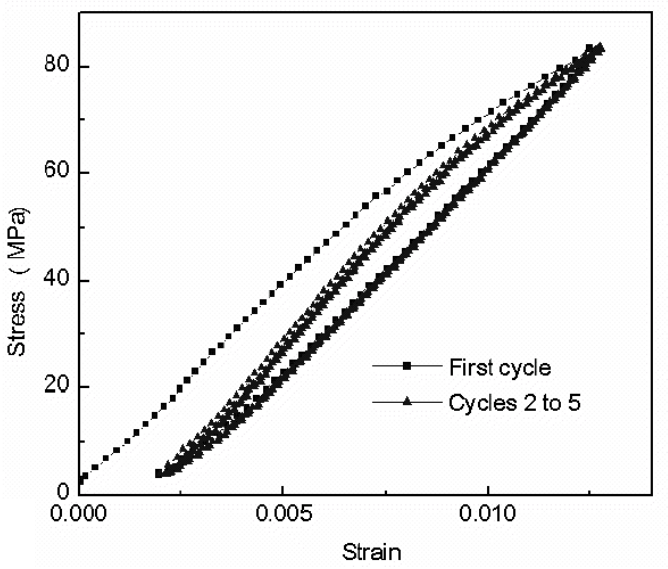

Figure 1: Compressive cyclic loading-unloading stress-strain curves of polycrystalline graphite at room temperature at ~ 80 MPa. In order to maintain sample alignment, the minimum stress in all tests was about 1–3 MPa [2].

increased as the square of the applied stress – a result that has to date also not been understood. Furthermore, excellent agreement between the micro- and macro tests is observed.

Experimental

Natural graphite single crystals of ≈ 1 to 2 mm in size were cleaved to expose, what appeared to be, defect free, atomically flat (0001) planes. To ensure that the sample surfaces were normal to the indenting direction, the crystals were mounted using a conductive epoxy on a steel ball that was attached to a specially made sample holder. The sample surface was leveled by rotating the steel ball to the correct inclination; this was done under an optical microscope. Once the correct inclination was obtained, the steel ball was tightened to fix the sample in that orientation.

Nanoindentations were performed with a MTS nanoindenter (XP®) using a 13.5 μm radius hemispherical diamond tip. The experiments were carried out under load control up to maximal loads of 2, 5, 10, 20, 50, 100, 200 and 400 mN. The loading rate was 0.6 mN/s. To study the effect of cycling, typically multiple – mostly 5 - indentations were carried out on the same location to a given load. To discount any experimental artifacts, similar tests were carried out in fused silica and sapphire at the above loads for comparison.

The first indents usually resulted in permanent residual displacements. To correct for this displacement, the residual displacements after the first indents were added to the second and subsequent loadings, in other words, the unloading curves on the second and subsequent loadings were forced to coincide. The corrected or shifted load/displacement curves were then converted to stress/strain curves [3-10]. The stress here is the normal contact stress, $P/\pi a^2$, and the strain is given by a/R, where P is the applied load, a is the contact area radius and R is the radius of the indenter.

A graphite block (Grade ISO-63, Toyo Tanso USA, Troutdale, OR) with a density of 1.83 Mg/m^3 and a compressive strength of 181 MPa was machined into cylinders 9.7 mm in diameter and 31 mm high. The cylinders were cyclically compressed in load control mode at a loading rate of 420 N/s which corresponds to a nominal strain rate of ~ 8.8×10^{-4} s^{-1}. The strain was measured by an MTS axial extensometer (25 mm gauge length) attached to the sample. In order to maintain sample alignment, the minimum stress in all tests was about 1–3 MPa. The results of this test are shown in Fig. 1.

Results and Discussion

Typical nanoindentation load-displacement curves indented along the 0001 direction (i.e. normal to the basal planes) to 200 mN are shown in Fig. 2a. The fist indent has a permanent deformation, but the repeated loadings on the same location at loads resulted in excellent cycle-to-cycle reproducibility. The areas of the second and subsequent loops are less than the first signifying hardening. The majority of the hardening occurs between the first and second loadings (see below). All these

observations are further confirmed when the same data are converted to stress/strain curves (Figs. 2b).

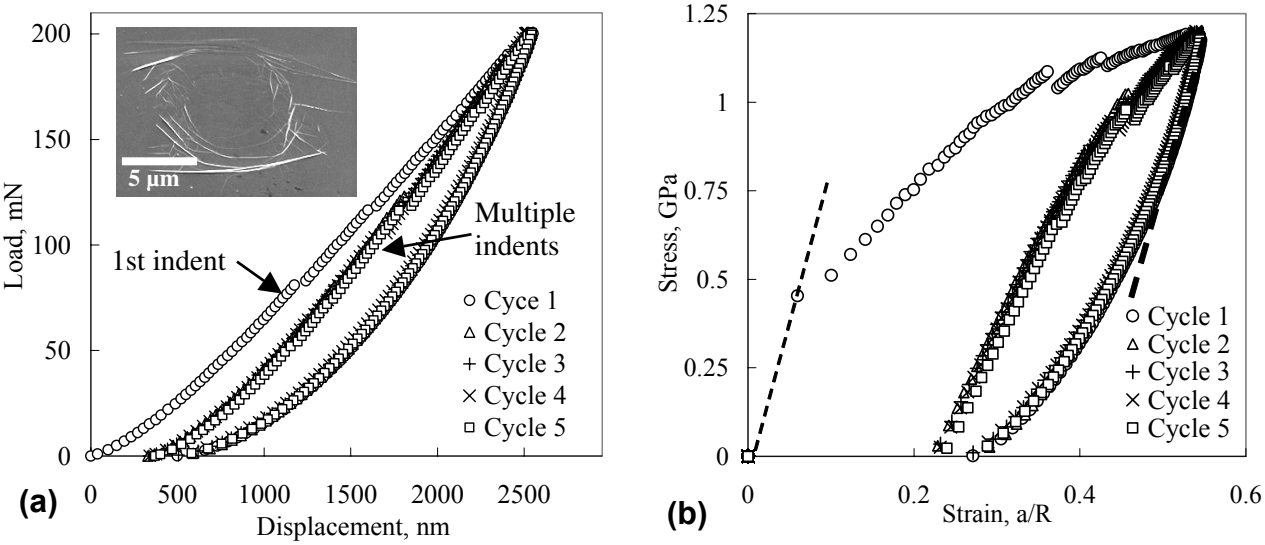

Figure 2: a) Load vs. depth-of- indentation response of graphite single crystals loaded along the 0001 direction to 200 mN. The first indent results in an open loop but subsequent indents encompass a smaller area. Inset shows SEM micrograph of indented area. (b) Stress/strain curves for results shown in a. The first loop is open, but subsequent loops are almost fully reversible. A dotted straight line drawn during initial unloading corresponds very well to the elastic loading slope.

Initially the response is linear elastic with a modulus assumed to be 36.5 GPa. Yielding occurs at a stress level around 0.4 GPa. Beyond the yield point hardening occurs with a rate that is linear with strain. At lower loads (5mN or 0.4 GPa and lower), the response is fully reversible hysteretic even in the first cycles with no hardening observed. The stress-strain curves could not be extracted reliably however, at low strain levels due to noise in the data.

The areas encompassed by the hysteresis loops in the stress-strain curves are a measure of the energy dissipated during each cycle, Wd. A log-log plot of Wd versus stress, s, is shown in Fig. 3. The excellent agreement between the values of Wd measured on bulk samples and those from nanoindentation experiments is gratifying. Also included in Fig. 3 are the results for Ti_3SiC_2 [11,12]. Note that a simple energy analysis predicts a theoretical slope of ~ 2 [12]. A least squares fit of the graphite data in Fig. 3 yields a slope of 1.96 with an R^2 value of > 0.99.

At higher loads (≈ 400 mN), the indents resulted in massive pop-ins of the order of 60 μm. Typical secondary FESEM micrographs of indentations made at 400 mN are shown in Fig. 4. The indentation locations appear as deep craters surrounded by defoliated graphene sheets. The center of the craters is comprised of a multitude of micron and submicron grains of random orientations. Evidence for kink boundaries (Fig. 4b) and the massive rotation of the lattice planes is unambiguous and ubiquitous. Interestingly, the symmetry of the indentations made with the spherical indenter is 6-fold (see white dotted hexagon in Fig. 4). This behavior is typical for spherical indentions of single crystals and has been also observed for Si and other materials.

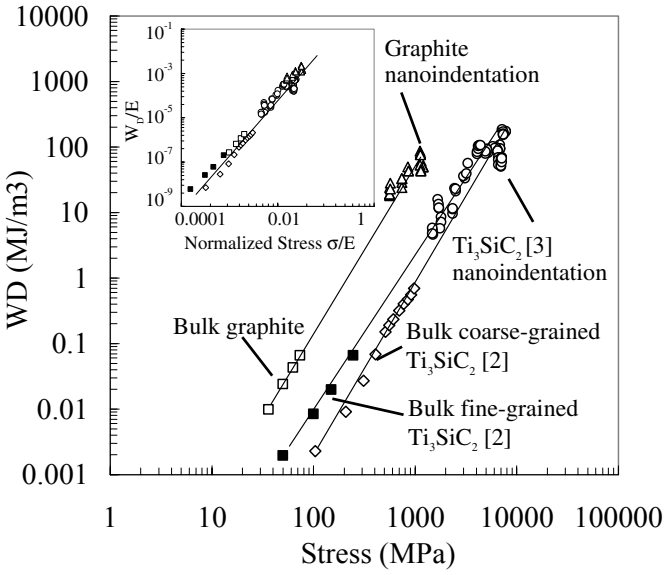

Figure 3**:** Log- log plot of energy dissipated per cycle, W_d, versus maximum stress for graphite. The results at lower stresses were obtained from Fig. 1; at higher stresses they were obtained from nanoindentation tests. The agreement is good despite the over 6 orders of magnitude range in W_d. The results for Ti_3SiC_2 [12] are also shown for comparison. Inset shows normalized results of work done vs. stress, normalized results of work done versus stress, normalized with the modulus along the loading direction (i.e., 36.5 GPa for graphite).

As this paper makes clear, there are many similarities between the deformations of Ti_3SiC_2 and graphite. To understand the response of the latter it is vital to review our understanding of the deformation of the former. Recently we have shown that polycrystalline samples of Ti_3SiC_2 cyclically loaded in compression at room temperature, to stresses up to 1 GPa, fully recover upon the removal of the load, while dissipating about 25% of the mechanical energy [11]. The stress-strain curves outline fully reversible, reproducible, rate-independent, closed hysteresis loops whose shape and extent of energy dissipated are strongly influenced by grain size, with the energy dissipated being significantly larger in the coarse-grained material. This phenomenon was attributed to the formation and annihilation of incipient and regular kink bands (see below). The same mechanism has also recently been proposed to explain the fully reversible and hardening behavior of Ti_3SiC_2 [12] and mica [13] surfaces indented with a 13.5 μm spherical indenter.

Given the critical importance of kink bands (KB) to this work it is crucial to briefly review the theory of their formation. Frank and Stroh [14] proposed a model in which pairs of dislocations of opposite sign nucleate and grow at the tip of a thin elliptical kink – henceforth referred to as a subcritical kink - with dimensions, 2α and 2β, such that α >>

β. The precise mechanism responsible for kink nucleation has to date not been identified.

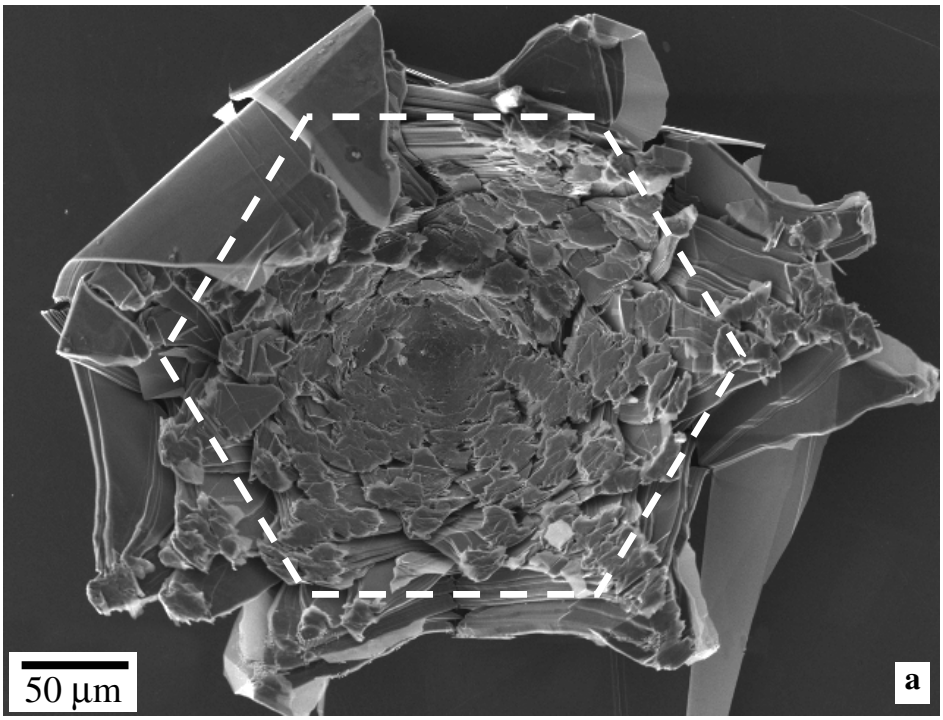

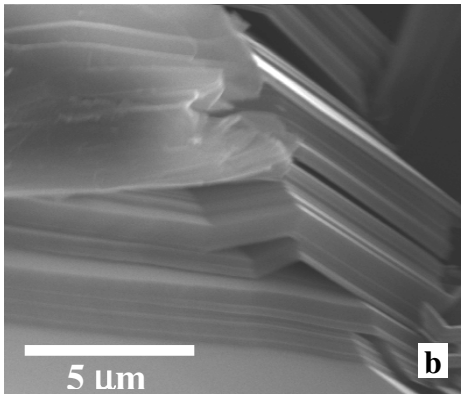

Figure 4**:** FESEM secondary micrographs of, a) spherical nanoindentation at 400 mN, the damage crater has a 6 fold symmetry (denoted by a dotted hexagon) b) Higher magnification of a focusing on edge of the indentation crater clearly showing the formation of kink bands and delaminations. Note such features cannot be formed by any other process.

However, by assuming the local stress needed to form a dislocation pair to be ~ G/30, where G is the shear modulus, it can be shown that at a critical kinking angle, $\gamma \approx$ 5-6°, the remote stress, τ_c, needed to render a subcritical KB unstable depends on α, and is given by [14]:

$$\tau_c \geq \sqrt{\frac{2bG^2\gamma\ln(1/\gamma)}{\alpha\pi^2(1-\nu)^2}}$$

where G, ν and b are, respectively, the shear modulus, Poisson's ratio and the Burgers vector. α is the domain size available for the creation of the IKB. According to Eq. 1 the smaller α or the volume available for kinking the larger the stresses required to form a kink. This is a crucial result because it explains the hardening observed (see below).

Frank and Stroh's model is two-dimensional and as such assumed that once a subcritical KB became critical, it would immediately extend to the free surface resulting in two parallel, mobile non-interacting dislocations walls. It is the repetition of this process that results in the generation of new dislocation walls whose coalescence form the KB's. The idea that a kink band can reach a grain boundary and not dissociate was not considered, but as discussed in this paper, it is crucial. As defined in this, and previous work [11-13], an incipient kink band or IKB is one in which the near parallel walls of opposite sign dislocations are undissociated i.e. still attracted to each other, which insures that when the load is removed the IKB's would be annihilated.

Fully reversible nanoindentation hysteretic loops have been observed in glassy carbons with nanometer sized grains [15] and CDCs [16]. In the case of glassy carbons, such a response is also observed with sharp indenters such as cube corner indenters. The reversible nature of the indents was explained in terms of the *reversible* slip of graphene planes in the nanometer grains [17] and the hysteresis was attributed to sliding friction between the layers due to the compressive stresses [15,18]. More recently, it has been suggested that dislocation pileups may be responsible [17]. Interestingly enough, pileups were our initial explanation for the results obtained on Ti_3SiC_2 [11]. That explanation was rejected, however, because it failed to account for the reversible nature of the deformation. The results of this work suggest the origin of the loops obtained in the porous carbons is the formation of IKB's and KB's.

The loss factors or damping in graphite are large compared to metals. This has been explained by invoking the dominance of shear processes and the presence of very high densities of glissile dislocations [1]. Here again, the presence of dislocations *per se* does not lead to large damping, if for e.g. these dislocations *entangle* as in the case for metals. A more plausible explanation is the one we propose, viz. the relatively large distances over which the basal plane dislocations can travel unhindered.

When the results shown in Fig. 3 are normalized by the appropriate elastic constants (36.5 GPa for graphite and 325 GPa for Ti_3SiC_2) they fall on a universal curve (inset in Fig. 3). The results for mica also fall on the same curve, providing compelling evidence that the underlying atomic mechanisms for all three solids are identical. The excellent agreement – over ~ 5 orders of magnitude in W_d - between the extrapolation of results obtained on bulk samples and those obtained from the nanoindentation stress/strain curves is noteworthy and gratifying. The agreement is even more remarkable when the differences in the definitions of stress and strain between the uniaxial case and those extracted from the nanoindentations experiments are considered. In sharp contradistinction to metals, the energy dissipated or damping capacity *increases* as σ^2 (Fig. 3). This observation alone is impossible to reconcile with the mere presence of dislocations, if the latter are allowed to entangle.

A long-standing mystery in the deformation of graphite has been the fact that when the sample dimensions are of the order of the microstructural features the compressive strengths decrease with decreasing sample size. Several explanations have been proposed [see references in Ref. 1]. The formation IKBs and KBs can easily explain these observations. The "yield" or deformation stresses in Ti_3SiC_2 are a strong function of constraining stresses; increasing the latter greatly enhances the former [12]. It is thus not unreasonable to conclude that the same occurs in graphite. This rationale is consistent with the observation that radial confining pressures increase the compressive strengths of some graphites [19]. The results of this work, however, are probably the most compelling demonstration of this fact; the stresses sustained under the indenter are, in some cases, of the order of 1 GPa; a value that is about an order of magnitude higher than typical compressive strengths of polycrystalline graphites that range from 30 to 100 MPa.

Since the nanoindentation experiments were carried out on a single crystal, the volumes probed were, more likely than not, perfect; a conclusion consistent with the fact that the yield point is ~ G/30. In the bulk samples, on the other hand, a multitude of grains are probed and the nucleation of the kink bands – a process that is currently not understood – occurs stochastically and over a distribution of stresses. Note that in all cases the local shear stresses needed to from a dislocation pair must be of the order of G/30.

To date, it has been shown that the $M_{n+1}AX_n$ (where n = 1 to 3 and M is an early transition metal, A is an A-group element and X is either C and/or N) family of ternary layered carbides and nitrides [12], and most probably ice [20] are all KNE solids. Even more recently it has been shown that mica, and by extension presumably most other layered silicates, are KNE solids [13]. Furthermore it has been shown that the nonlinear elastic, hysteretic and discrete memory elements of nonlinear mesoscopic elastic (NME) solids [21] are nothing but IKBs.

Conclusions

In this work we present a kinking-based model that explains the response of graphitic surfaces, indented with a 13.5 μm radius spherical nanoindenter loaded along the c-axis, and polycrystalline samples to mechanical stress. The model also can account for many aspects of the deformation of graphite that to date been resisted explanation. The key to the model is the identification of a fully reversible hysteretic element – labeled incipient kink bands - comprised of near parallel dislocation walls that are strongly attractive. As long as the stress level is insufficient to sunder the IKB's the mechanical response is characterized by fully reversible hysteretic loops. At higher stresses, the IKB's give way to mobile dislocation walls that result in plastic strain. The ultimate coalescence of these walls into kink boundaries that reduce the domain size, account for the cyclic hardening observed.

Because the dislocations are confined to the basal planes, they do not entangle, and thus can move reversibly over relatively large distances. This feature results in the dissipation of substantial amounts of energy per cycle and accounts for the increase in

energy dissipated with increased stress levels. The proposed mechanism is valid over a wide range of stresses as seen from the work done vs. stress plots that show very good agreement over more than 4 orders of magnitude, between nanoindentations and simple compression experiments.

References

[1] Kelly BT. Physics of Graphite. Applied Science Publishers, London, 1981.
[2] M.W. Barsoum, A. Murugaiah, S.R. Kalidindi, T. Zhen and, Y. Gogotsi, Kink Bands, Nonlinear Elasticity and Nanoindentations in Graphite *Carbon in press*.
[3] Iwashita N, Swain MV, Field JS, Ohta N, Bitoh S. Elasto-plastic deformation of glass-like carbons heat-treated at different temperatures. Carbon. 2001; 39: 1525-1532.
[4] Iwashita N, Field JS, Swain MV. Indentation hysteresis of glassy carbon materials. Phil. Mag. A 2002; 82: 1873-1881.
[5] Katagiri G, Ishida H, Ishitani A. Raman spectra of graphite edge planes. Carbon 1988; 26: 565-571.
[6] Tabor D. Hardness of Metals. Clarendon Press, Oxford, United Kingdom, 1951.
[7] Lawn BR, Padture NP, Cai H, Guiberteau F. Making ceramics “Ductile”. Science 1994; 263: 1114.
[8] Guiberteau F, Padture NP, Lawn BR. Effect of grain size on hertzian contact damage in alumina. J. Amer. Cer. Soc. 1994; 77: 1825.
[9] Swain MV. Mechanical property characterisation of small volumes of brittle materials with spherical tipped indenters. Mat. Sci. and Engg., A 1998; 253: 160.
[10] Gogotsi Y, Dominich V. High Pressure Surface Science and Engineering, Institute of Physics, 2004
[11] Barsoum MW, Zhen T, Kalidindi S, Radovic M, Murugaiah A. Dislocation based fully reversible compression of Ti3SiC2 up to 1 GPa. Nature Materials 2003; 2: 107-111.
[12] Murugaiah A, Barsoum MW, Kalidindi SR, Zhen T. Spherical nanoindentations in Ti3SiC2. J. of Mat. Res. in press.
[13] Barsoum MW, Murugaiah A, Kalidindi SR, Zhen T. Kinking Nonlinear Elastic Solids, Nanoindentations and Geology. Phy. Rev. Lett. In press.
[14] Frank FC, Stroh AN. On the theory of kinking. Proc. Phys. Soc. 1952; 65: 811.
[15] Iwashita N, Swain MV, Field JS, Ohta N, Bitoh S. Elasto-plastic deformation of glass-like carbons heat-treated at different temperatures. Carbon. 2001; 39: 525- 1532
[16] Gogotsi Y, Welz S, Ersoy DA, McNallan MJ. Conversion of SiC to crystalline diamond structured carbon. Nature 2001; 411: 283-287.
[17] Sakai M, Nakano Y, Shimizu S. Elastoplastic indentation on heat-treated carbons. J. Am. Cer. Soc. 2002; 85: 1522–1528.
[18] Field JS, Swain MV. The indentation characterization of the mechanical properties of various carbon materials: glassy carbon, coke and pyrolytic graphite. Carbon 1996; 34: 1357.
[19] Taylor R, Brown R, Gilchrist KE, Hodds AT, Kelly BT, Morris F, Hall E. Carbon1967; 5: 519.
[20] M.W. Barsoum, M. Radovic, P. Finkel, and T. El-Raghy, “Ti_3SiC_2 and Ice”, Appl. Phys. Lettrs. **79,** 479 (2001).
[21] R. A. Guyer and P. A. Johnson, Physics Today, April (1999). Feature article.